

STEADY STATE SOLUTION OF FINITE HYDROSTATIC DOUBLE-LAYERED POROUS JOURNAL BEARINGS WITH TANGENTIAL VELOCITY SLIP INCLUDING PERCOLATION EFFECT OF POLAR ADDITIVES OF COUPLED STRESS FLUIDS

SHITENDU SOME^{a1} AND SISIR KUMAR GUHA^b

^{ab}Department of Mechanical Engineering, Indian Institute of Engineering Science and Technology, Shibpur, India

ABSTRACT

A theoretical investigation has been made into the steady state characteristics of finite externally pressurised double-layered porous journal bearings lubricated with coupled stress fluid with tangential velocity slip at the fine porous interface. The analysis takes into account of the tangential velocity slip based on the Beavers-Joseph criterion. Moreover, the present study includes the effects of percolation of the polar additives (microstructures) into the coarse and fine layers of porous medium. The most general modified Reynolds type equation has been derived for a porous journal bearing lubricated with coupled stress fluids. The governing equations for flow in the coarse and fine layers of porous medium incorporating the percolation of polar additives of lubricant and modified Reynolds equation in the film region are solved simultaneously using finite difference method, satisfying appropriate boundary conditions. The effects of slip, speed parameter, percolation factor and coupled stress parameter on the static characteristics in terms of load capacity, attitude angle and frictional parameter has been investigated. The results are exhibited in the form of graphs which may be useful for design of such bearing.

KEYWORDS: Coupled Stress, Double-Layered Hydrostatic Porous Journal Bearing, Percolation, Steady State, Velocity Slip.

Externally pressurized bearings find various applications in industry for higher load carrying capacity and frictionless running of the bearings. But externally pressurized bearings are multi-recess capillary or orifice-compensated bearings, which are very costly and complicated in design and sometimes it is very difficult to get uniform distribution of pressurized lubricant in the film region resulting pressure drop in the film region and variance of pressure. This drawback can be eliminated efficiently by using porous materials in bearings for hydrostatic lubrication, the lubricant is able to flow through a large number of pores; so, a uniform pressure distribution in film region and equal pressure bleeds from the porous surface ensuing a more even distribution of pressure in film region. In case of Newtonian lubricant, a higher threshold of stability is achieved by the porous bearing. For these practical aspects and low cost, porous bearings find various applications in industries.

Research on the porous bearings using Newtonian fluid as a lubricant initiated in the late 1950s. First mathematical model on hydrodynamic lubrication on porous bearings was presented by Morgan and Cameron [1], but it was Howarth [2] who was first carried out theoretical and experimental investigation on externally pressurized porous bearings. Since then several investigations in this field have done by many researchers [3-6]. But these studies were based on conventional porous bearings.

Disadvantages of the conventional porous bearings are less stability and low load carrying

capacity due to the seepage into the bearing wall. For increasing the load carrying capacity and stability, double layered porous bearings are better than the conventional porous bearings, because double layered porous bearings restrict the seepage into porous walls. It is possible to control the fluid flow through the two-layered structure such that over 90–95% of the pressure drop occurs across the thin fine layer, even with its thickness of only 5–10% of the coarse layer [7,8]. Heinzl [9] and Okano [10] considered that the double layered porous bearings could be used for enhancing stability. Saha and Majumder [7] presented that two layered porous bearings represent better load carrying capacity and stability than conventional porous bearings. Kumar et al. [11] theoretically investigated the steady state characteristics of finite hydrostatic double layered porous oil journal bearing. But these studies on conventional porous bearings or double layered porous bearings were confined to Newtonian lubricant.

In the recent years the field of lubrication has enriched due to the development of lubricating effectiveness of non-Newtonian fluids as in the most of the practical usages. Meanwhile various micro continua theories [12-14] to properly describe the rheological behavior of non-Newtonian fluids, mainly the polymer-thickened oils or lubricants blended with the additives. Among various micro continuum theories, Stokes coupled stress fluid model [12] has been widely used for its mathematical simplicity. A few researchers [15-18] have implemented the non-

Newtonian approach into their studies, but these studies were confined to conventional porous bearings.

Maximum theoretical investigations that have been established on double-layered porous bearing so far, maximum investigators solved the Reynold's equation using no slip boundary condition at the porous wall surface. Only Kumar et al. [11] have considered the velocity slip in their study based on the Beavers and Joseph model [19], but their work was confined to Newtonian model. So, it is necessary to consider the velocity slip in case of double-layered porous bearing with non-Newtonian lubricant. In case of non-Newtonian lubrication of the porous bearing, percolation effect of the polar additives is one of the most important phenomenon. But maximum investigators assumed that the polar additives present in the non-Newtonian lubricant in the film region do not percolate. Naduvinamani et al. [16] and Guha [18] have considered the percolation effect in their studies, but these studies were based on the conventional porous bearings. However, there is no literature available so far that addresses the theoretical analysis of the steady state characteristics of hydrostatic double-layered porous bearings with tangential velocity slip including percolation effect of polar additives of coupled stress fluids.

The aim of the present investigation is to solve the governing equation for hydrostatic double-layered porous bearings with tangential velocity slip and percolation effect of the coupled stress lubricant. The effects of slip, speed parameter, percolation factor and coupled stress parameter on the static characteristics in terms of load capacity, attitude angle and frictional parameter has been investigated. The results are exhibited in the form of graphs which may be useful for design of such bearing.

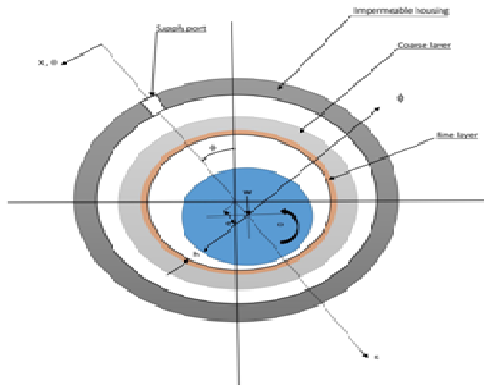


Figure 1: Schematic diagram of two-layered porous journal bearing

Theoretical Analysis

In the porous region (both coarse and fine layers), the velocity components of a coupled stress fluid are governed by the modified form of Darcy's law [20], Which accounts for the additives effects in the pores and can be represented as

$$u' = - \frac{k_x}{\mu(1 - \gamma_x)} \frac{\partial p'}{\partial x}$$

$$v' = - \frac{k_y}{\mu(1 - \gamma_y)} \frac{\partial p'}{\partial y}$$

$$w' = - \frac{k_z}{\mu(1 - \gamma_z)} \frac{\partial p'}{\partial z}$$

Where k_n is the permeability coefficient of porous matrix in $n = x, y, z$ directions, γ_n represents the ratio of micro-structure size to the pore size in $n = x, y, z$ directions and is known as percolation factor as defined by

$$\gamma_n = \frac{\eta}{\mu k_n} = \frac{l^2}{k_n} \text{ where } l = \sqrt{\frac{\eta}{\mu}}$$

The non-dimensional governing equations of pressure in porous layers for an anisotropic bearing can be written as follows:

For the coarse layer

$$\chi_{xc} \bar{K}_{xc} \frac{\partial^2 \bar{p}'_c}{\partial \theta^2} + \left(\frac{R}{H}\right)^2 \frac{\partial^2 \bar{p}'_c}{\partial \bar{y}^2} + \left(\frac{D}{L}\right)^2 \chi_{zc} \bar{K}_{zc} \frac{\partial^2 \bar{p}'_c}{\partial \bar{z}^2} = 0 \dots \dots \dots (1)$$

For the fine layer

$$\chi_{xf} \bar{K}_{xf} \frac{\partial^2 \bar{p}'_f}{\partial \theta^2} + \left(\frac{R}{H}\right)^2 \frac{\partial^2 \bar{p}'_f}{\partial \bar{y}^2} + \left(\frac{D}{L}\right)^2 \chi_{zf} \bar{K}_{zf} \frac{\partial^2 \bar{p}'_f}{\partial \bar{z}^2} = 0 \dots \dots \dots (2)$$

Non-dimensional modified Reynold's equation in the clearance region of porous bearing lubricated with coupled- stress fluid including the velocity slip and the additives effect in the pores for steady state analysis is

$$\begin{aligned} \frac{\partial}{\partial \theta} \left[f(\bar{h}, \sigma_x, \bar{l}, \gamma_{xf}) \frac{\partial \bar{p}}{\partial \theta} \right] + \left(\frac{D}{L}\right)^2 \frac{\partial}{\partial \bar{z}} \left[f(\bar{h}, \sigma_z, \bar{l}, \gamma_{zf}) \frac{\partial \bar{p}}{\partial \bar{z}} \right] \\ = A_s \frac{\partial}{\partial \theta} \{ \bar{h} (1 + \xi_{0x}) \} \\ + \frac{\beta}{\mu(1 - \gamma_{yf})} \frac{\partial \bar{p}_f}{\partial \bar{y}} \Big|_{\bar{y}=0} \dots \dots \dots (3) \end{aligned}$$

Where

$$f(\bar{h}, \sigma_n, \bar{l}, \gamma_{nf}) = \bar{h}^3 \left\{ 1 + \frac{\xi_n}{(1 - \gamma_{nf})} \right\} - 6\bar{h}^2 \bar{l} \xi_{0n} \tanh\left(\frac{\bar{h}}{2\bar{l}}\right) - 12\bar{l}^2 \left\{ \bar{h} - 2\bar{l} \tanh\left(\frac{\bar{h}}{2\bar{l}}\right) \right\}$$

$$\xi_n = \frac{3\{2\alpha + \sigma_n \bar{h}(1 - \gamma_{nf})\}}{\sigma_n(\bar{h} + \alpha \sigma_n \bar{h}^2)}, \quad \xi_{0n} = \frac{1}{1 + \alpha \sigma_n \bar{h}},$$

$$\chi_{nc} = \left(\frac{1 - \gamma_{nc}}{\bar{K}_{nc} - \gamma_{nc}} \right),$$

$$\chi_{nf} = \left(\frac{1 - \gamma_{nf}}{\bar{K}_{nf} - \gamma_{nf}} \right), \quad n = x, z$$

Method of Solution

The governing equations (1-2) for flow in the coarse and fine layers of porous medium incorporating the percolation of polar additives of lubricant and modified Reynolds equation (3) in the film region are written simultaneously in finite difference method using central difference scheme and then solved by the Gauss-Seidel iteration method with successive over relaxation scheme, satisfying appropriate boundary conditions [7,11].

A three-dimensional grid pattern with a uniform grid size is adopted for each layer with 50 (circumferential direction), 14 (axial direction), 14 (radial direction) divisions. The convergence criterion adopted for pressure is $|(1 - \sum \bar{p}_{old} \sum \bar{p}_{new})| \leq 0.0001$. The convergence criterion was reduced up to 0.00001 and no appreciable change in results was observed. Hence it was concluded that the present results are fairly accurate.

Steady State Characteristics

Once the differential equations are solved by satisfying the boundary conditions and convergence limit for the film pressure distribution, the steady state characteristics can be obtained as follows:

Load Carrying Capacity

Load carrying capacity of the bearing can be obtained by integrating the film pressure around the circumference and along the total length of the bearing. Where \bar{W}_r and \bar{W}_t are the non-dimensional component of load carrying capacity along the radial and tangential direction.

$$\bar{W}_r = \frac{W_r}{LRp_s} = - \int_0^1 \int_0^{\theta_2} \bar{p} \times \cos \theta \cdot d\theta \cdot d\bar{z} \dots \dots \dots (4)$$

$$\bar{W}_t = \frac{W_t}{LRp_s} = + \int_0^1 \int_0^{\theta_2} \bar{p} \times \sin \theta \cdot d\theta \cdot d\bar{z} \dots \dots \dots (5)$$

Non dimensional total load-carrying capacity

$$\bar{W} = [\{\bar{W}_r\}^2 + \{\bar{W}_t\}^2]^{1/2} \dots \dots \dots (6)$$

With the help of non-dimensional load component, attitude angle can be obtained by using the following relation

$$\phi_0 = \tan^{-1} \left[\frac{\bar{W}_t}{\bar{W}_r} \right] \dots \dots \dots (7)$$

Once the pressure distribution is obtained numerically for all the mesh points, the load-carrying capacity can be calculated numerically using Simpson's 1/3 rule.

Coefficient of Friction

In oil film porous bearing, the friction phenomenon exhibited in two regions: 1) non-cavitation region 2) cavitation region.

Non-dimensional frictional force for the non-cavitation region where oil film extending from $\theta = 0$ to $\theta = \theta_2$ is given by

$$\bar{F}_{s1} = \frac{F_{s1}}{LCp_s} = \int_0^1 \int_0^{\theta_2} \left[\frac{1}{\bar{h}} (1 - \xi_{0x}) + \frac{\partial \bar{p}}{\partial \theta} \left(\frac{\bar{h}}{2} \left(1 + \frac{\xi_x}{3(1 - \gamma_{xf})} \right) - \bar{l} \xi_{0x} \tanh\left(\frac{\bar{h}}{2\bar{l}}\right) \right) \right] d\theta \cdot d\bar{z} \dots \dots \dots (8)$$

Non-dimensional frictional force in the cavitation region, where there is a discontinuous mixture of oil, vapour etc., extending from $\theta = \theta_2$ to $\theta = 2\pi$ is given by

$$\bar{F}_{s2} = \frac{F_{s2}}{LCp_s} = \int_0^1 \int_{\theta_2}^{2\pi} \left(\frac{\bar{h}_{cav}}{\bar{h}} \right) \left[\frac{1}{\bar{h}} (1 - \xi_{0x}) + \frac{\partial \bar{p}}{\partial \theta} \left(\frac{\bar{h}}{2} \left(1 + \frac{\xi_x}{3(1 - \gamma_{xf})} \right) - \bar{l} \xi_{0x} \tanh\left(\frac{\bar{h}}{2\bar{l}}\right) \right) \right] d\theta \cdot d\bar{z} \dots \dots \dots (9)$$

Total frictional force $\bar{F}_s = \bar{F}_{s1} + \bar{F}_{s2}$

Friction variable is given by $\mu_f \left(\frac{R}{c} \right) = \frac{\bar{F}_s}{\bar{W}}$

Once the pressure distribution is obtained numerically for all the mesh points, the load-carrying capacity, attitude angle, coefficient of friction can be calculated numerically using Simpson's 1/3 rule for numerical integration and three- point backward or forward difference rule is applied for differentiation.

RESULTS AND DISCUSSION

It is evident from equations (1) and (2) applicable for the double layered porous bush and a modified Reynolds type equation denoted by equation (3) for the film region that the film pressure distribution depends on the parameters namely, $L/D, H/R, \alpha, \beta, \Lambda_s, K_{nc}, K_{nf}, (n = x, z), \gamma_{nc}, \gamma_{nf} (n = x, y, z), \varepsilon_0, \bar{l}$. A parametric study has been carried out for all the above mentioned parameters excepting $L/D, K_{ic}$ and $K_{if}, (i = x, z)$ which has been fixed at 1.0. A wide ranges of \bar{l} values (0 - 0.7) and γ_{yf} values (0.1- 0.7) have been considered for the present analysis.

In the present study, the inclusion of two non-dimensional parameters viz. α and $s_n = \frac{1}{\alpha\sigma_i}$ imposes the condition of slip ($n = x, y$). The slip parameter, s_n is a non- dimensional parameter consisting of slip coefficient, α and permeability factor, σ_i which is expressed as

$$\sigma_n = \frac{C}{\sqrt{K_n}} = \frac{1}{\bar{l}} \sqrt{\gamma_n K_n} \quad (n = x, z)$$

Where s_n is a function of slip coefficient, α , permeability coefficient, K_i , percolation factor, γ_n and coupled stress parameter, \bar{l} . Therefore, the effect of slip is understood through the slip coefficient, α and also by the inclusion of the permeability factor, σ_i . Furthermore, the no slip condition is attained by setting α to infinity which consequently tends s to zero.

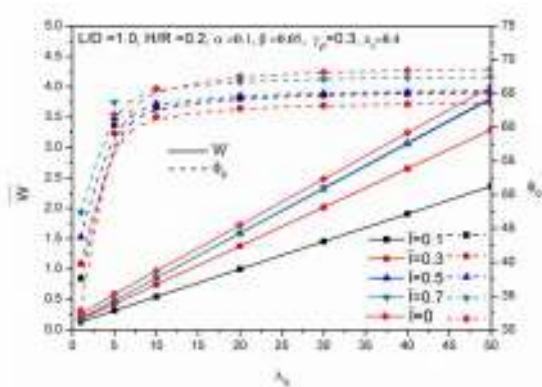


Figure-2: Variation of load and attitude angle with Λ_s for various values of \bar{l}

Figure-2 shows the variation in the non-dimensional load carrying capacity and attitude angle of a double-layered porous bearing having isotropic permeability as a function of bearing number, Λ_s for various values of coupled stress parameter, \bar{l} . An analysis of the figure reveals that as the bearing number increases, the non-dimensional load capacity increases for a particular value of \bar{l} . At a particular value of Λ_s , the effect of \bar{l} is to increase the load capacity. The rate with which the load capacity increases as Λ_s increases is higher for higher values of \bar{l} . The load capacity for Newtonian lubricant is higher than those in case of the coupled stress fluids.

Figure-2 also shows the variation of attitude angle with respect of Λ_s for various values of \bar{l} . It is observed from the figure that attitude angle increases with Λ_s for a particular value of \bar{l} . This increases is more predominant at lower values of Λ_s . As \bar{l} is increased, attitude angle is found to decrease at lower values of Λ_s , but at higher values of Λ_s , such effect is not observed. In case of Newtonian fluid, attitude angle is found to be above the values of coupled stress fluids at higher values of Λ_s .

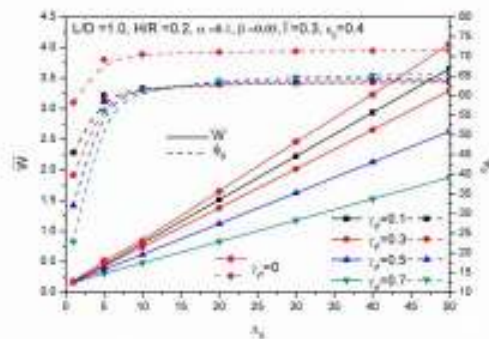


Figure-3: Variation of load and attitude angle with Λ_s for various values of γ_{yf}

Effect of bearing number Λ_s on the load capacity of bearing and attitude angle is shown in figure-3, when the percolation factor γ_{yf} is taken as a parameter. It is observed that the load capacity increases with Λ_s for a particular value of γ_{yf} . But a particular value of Λ_s , load capacity decreases with increase in γ_{yf} . This is due to fact that for a value of \bar{l} , an increase in γ_{yf} results in increase in the permeability factor, σ_{yf} in fine porous layer. Consequently, load capacity reduces due to increase in γ_{yf} irrespective of Λ_s values. The variation tendency of the load capacity with γ_{yf} at higher values of Λ_s becomes more

conspicuous. Variation of attitude angle with Λ_s is shown in the above figure, when γ_{yf} is taken as a parameter. Attitude angle is found to decrease with increase in γ_{yf} . It is further observed that beyond $\Lambda_s \approx 15$, the reverse trend of variation is observed. The load capacity for no-percolation condition is higher than those values for percolated condition at all values of Λ_s .

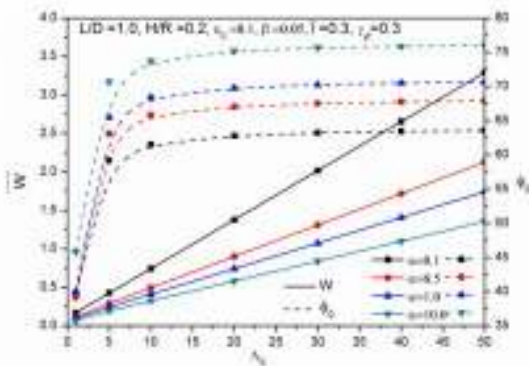


Figure-4: Variation of load and attitude angle with Λ_s for various values of α

Figure-4 exhibits the variation of load carrying capacity with respect Λ_s of for various values of α . It is observed that an increase in α reduces the load capacity for all values of bearing number, Λ_s . The effect of α on the load capacity is more significant at higher values of Λ_s . The effect of α on attitude angle is shown in the above figure. It is found that the effect of α is to increase the attitude angle at any value of Λ_s . However, the change of attitude angle with α is considerable at higher values of Λ_s .

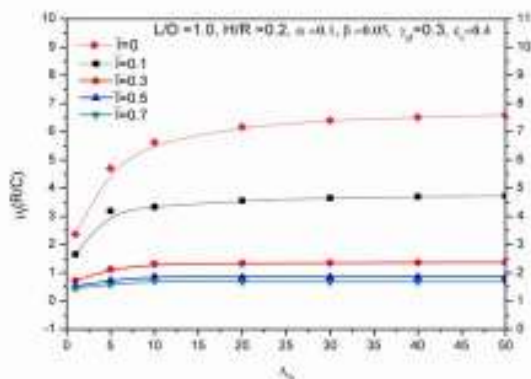


Figure-5: Variation of friction parameter with Λ_s for various values of \bar{l}

Friction parameter, $\mu_f(R/C)$ is shown in figure-5 as a function of Λ_s for various values of \bar{l} . It is found that, in general, the friction parameter increases

with Λ_s for a particular value of \bar{l} . The effect of \bar{l} , as found in the figure, is to reduce the frictional parameter for any Λ_s as \bar{l} increases. The decrease in frictional parameter become less prominent at higher values of \bar{l} at any value of Λ_s . The frictional parameter of bearing lubricated with Newtonian fluid ($\bar{l} \approx 0$) found to be higher than those values for bearing lubricated with coupled stress fluid for any values of Λ_s .

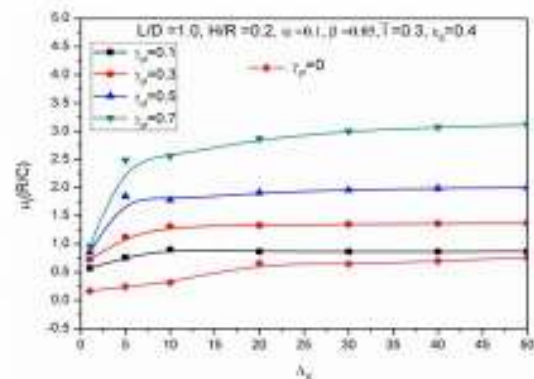


Figure-6: Variation of friction parameter with Λ_s for various values of γ_{yf}

The effect of γ_{yf} on the frictional parameter can be analysed from the figure-6. An increase in γ_{yf} increases the frictional parameter for any value of Λ_s . For a particular value of γ_{yf} , friction parameter increases with Λ_s and the increase becomes more predominant at lower values of Λ_s . The increasing tendency of the curves becomes more conspicuous as γ_{yf} is increased at any value of Λ_s .

The effect of α on the frictional parameter can be studied from the figure-7. Hence, too, it is observed that an increase in α increases the frictional parameter at any value of Λ_s . The increasing tendency of the curves at any value of Λ_s becomes more prominent as α is increased.

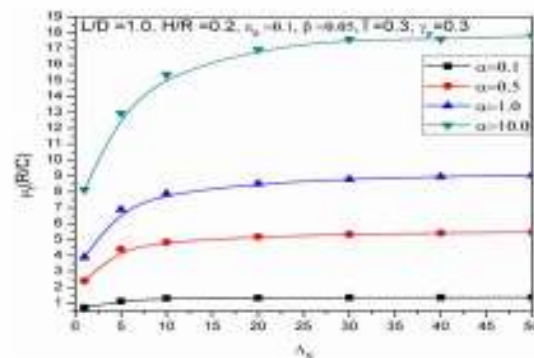


Figure-7: Variation of friction parameter with Λ_s for various values of α

In addition, the results obtained from the present study for variation of load capacity, attitude angle, frictional parameter with Λ_s for various values of β , have been shown in below chart:

Λ_s	β	\bar{W}	ϕ_0	$\mu_f \left(\frac{R}{C} \right)$
5	0.001	0.369158	61.46090	1.61002
	0.05	0.424961	59.17368	1.12453
	1	0.374257	33.07814	1.29263
10	0.001	0.735937	61.51622	1.33683
	0.05	0.741472	61.52375	1.31275
	1	0.514953	52.48225	1.87885
20	0.001	1.469445	61.54311	1.26911
	0.05	1.378149	62.80412	1.33235
	1	0.870550	68.82571	2.22051
30	0.001	2.202847	61.55102	1.25687
	0.05	2.015775	63.22719	1.34889
	1	1.189384	69.67404	2.13346
40	0.001	2.936357	61.55577	1.25263
	0.05	2.653832	63.42831	1.35912
	1	1.399590	71.95139	2.32330
50	0.001	3.669866	61.55863	1.25071
	0.05	3.292184	63.54271	1.36585
	1	1.609345	73.26615	2.52167

CONCLUSION

The effect of percolation and velocity slip on the steady state performance characteristics of finite hydrostatic double-layered porous bearing was discussed. The following conclusions are drawn on the basis of above theoretical investigation:

- 1) The effect of coupled stress parameter(\bar{l}) on the performance of hydrostatic doubled layered porous journal bearing is significant at higher values of bearing number(Λ_s). At a particular value of Λ_s , load carrying capacity and attitude angle increase with increase in \bar{l} . The friction variable decreases with the effect of coupled stress parameter. The load carrying capacity and attitude angle for Newtonian lubricant is higher than those in case of the coupled stress lubricant.
- 2) The effect of percolation factor(γ_{yf}) on the performance of hydrostatic doubled layered porous journal bearing is significant at higher values of bearing number(Λ_s). At a particular value of Λ_s , load carrying capacity decreases and frictional parameter increases with increase in γ_{yf} . Attitude

angle decrease with increase in γ_{yf} , but the reverse trend of variation is observed beyond $\Lambda_s \approx 15$. The Load carrying capacity and attitude angle for no percolation ($\gamma_{yf} \approx 0$) effect is higher than those in case of the percolation effect.

- 3) At a particular value of Λ_s , attitude angle and frictional parameter increase with increase in slip coefficient(α). But load carrying capacity decreases with increase in slip coefficient(α).

NOMENCLATURE

C	Radial clearance of the bearing.
D	Diameter of the bearing.
e	Eccentricity of the bearing.
\bar{F}_s	Dimensionless total frictional force on the journal surface.
h	Local film thickness.
\bar{h}	Dimensionless film thickness (h/C).
H	Thickness of the porous bush.
H_f, H_c	Thickness of the fine and coarse layers, respectively.
k_{xf}, k_{yf}, k_{zf}	Permeability coefficient of the fine layer along x,y,z direction, respectively.
k_{xc}, k_{yc}, k_{zc}	Permeability coefficient of the coarse layer along x,y,z direction, respectively.
$\bar{K}_{xf}, \bar{K}_{zf}$	Dimensionless Permeability coefficient of the fine layer, $k_{xf}/k_{yf}, k_{zf}/k_{yf}$, respectively.
$\bar{K}_{xc}, \bar{K}_{zc}$	Dimensionless Permeability coefficient of the coarse layer, $k_{xc}/k_{yc}, k_{zc}/k_{yc}$, respectively.
\bar{K}_{yc}	Dimensionless interlayer permeability coefficient, k_{yc}/k_{yf}
l	Characteristics length of additives.
\bar{l}	Dimensionless characteristics length of additives, $\bar{l} = l/C$.
L	Length of the bearing.
p_a	Ambient pressure.
p_s	Supply pressure.
\bar{p}_s	Dimensionless supply pressure, p_s/p_a
p	Local film pressure in bearing clearance.
\bar{p}	Dimensionless local film pressure in bearing clearance, p/p_s
p'_f, p'_c	Local film pressure in the fine and coarse layers, respectively.
\bar{p}'_f, \bar{p}'_c	Dimensionless local film pressure in the fine and coarse layers, $p'_f/p_s, p'_c/p_s$, respectively.

R	Radius of journal.
\bar{W}	Dimensionless total load carrying capacity.
\bar{W}_r, \bar{W}_t	Dimensionless components of load carrying capacity.
x, y, z	Cartesian coordinate axis along circumferential, radial, axial direction, respectively.
θ, \bar{y}, \bar{z}	Dimensionless coordinates, $\theta = \frac{x}{R}$, $\bar{y} = \frac{y}{H}$, $\bar{z} = \frac{z}{L}$
γ_n	Percolation factor in n -direction, $n = x, y, z$
γ_{nf}, γ_{nc}	Dimensionless percolation factor for fine and coarse layers, respectively, $n = x, y, z$
σ_n	Dimensional permeability factor, $\sigma_n = C/\sqrt{K_n}$, $n = x, z$
α	Slip coefficient.
μ	Coefficient of classical absolute viscosity of the lubricant.
η	Material constant with the dimension of momentum accounting for coupled stress.
Λ_S	Bearing number, $\Lambda_S = 6\mu\Omega R^2/p_s C^2$
β	Bearing feeding parameter, $\beta = 12k_y R^2/H C^3$
ξ_n	Slip function in n -direction, $n = x, z$
ξ_{0x}	Slip function defined by, $\xi_{0x} = 1/1 + \alpha\sigma_x \bar{h}$
χ_{nf}, χ_{nc}	Percolation function for fine and coarse layers in n -direction, $n = x, z$
ϕ_0	Attitude angle.
μ_f	Coefficient of friction.
ω	Angular velocity of journal rotation.
θ_2	Angular coordinates at which film cavitates.
ε_0	Eccentricity ratio, $\varepsilon_0 = e/C$

REFERENCES

- Morgan V.T. and Cameron A., 1957. Mechanism of lubrication in porous metal bearings. In: institution of Mechanical Engineers conference on lubrication and wear, London, 1:151–157.
- Howarth R.B., 1973. Optimum performance of externally pressurized porous thrust bearings. A S L E Transactions, 17:127-133.
- Chattopadhyay A.K. and Majumdar B.C., 1984. Steady state solution of finite hydrostatic porous oil journal bearings with tangential velocity slip. Tribol Int., 17:317–323.
- Chattopadhyay A.K. and Majumdar B.C., 1984. Dynamic characteristics of finite porous journal bearings considering tangential velocity slip. Trans ASME J Tribol., 106:534–6.
- Guha S.K., 1986. Study of conical whirl instability of externally pressurized porous oil journal bearings with tangential velocity slip. Trans ASME J Tribol., 108:256–61.
- Haque R. and Guha S.K., 2005. On the steady-state performance of isotropically rough porous hydrodynamic journal bearings of finite width with slip-flow effect. J. Mechanical Engineering Science., 219:1249-66.
- Saha N. and Majumdar B.C., Steady state and stability characteristics of hydrostatic two layered porous oil journal bearings. J Eng Tribol IMECHE, 218:99–108.
- Saha N. and Majumdar B.C., 2003. Stability of oil-lubricated externally pressurized two-layered porous journal bearings: a non-linear transient analysis. J Eng Tribol IMECHE, 217:223-228.
- Heninzi J., 1982. Aerostatisches Lager. German Patent De31 10712 A1, Munich.
- Okano M., 1991. Studies of externally pressurized porous gas bearings. Res Electrotech Lab, 952: 1-145.
- Kumar M.P., Samanta P. and Murmu N.C., 2015. Investigation of velocity slip effect on steady state characteristics of finite hydrostatic double-layered porous oil journal bearing. Proc IMechE Part J: J Engineering Tribology, 229(7):773–784.
- Stokes V.K., 1966. Couple-stresses in fluids. The physics of fluids, 9:1709-1715.
- Ariman T.T. and Sylvester N.D., 1973. Micro continuum fluid mechanics-a review. Int. J. Eng. Sci., 11:905-930.
- Ariman T.T. and Sylvester N.D., 1974. Application of micro continuum fluid mechanics. Int. J. Eng. Sci., 12:273-293.
- Naduvinamani N.B., Hiremathand P.S. and Gurubasavaraj G., 2001. Static and dynamic behaviour of squeeze-film lubrication of narrow porous journal bearings with coupled

stress fluid. Proc Instn Mech Engrs., **215**:45-62.

Naduvinnamani N.B., Hiremath P.S. and Gurubasavaraj G., 2001. Squeeze film lubrication of a short porous journal bearing with coupled stress fluids. Tribol Int., **34**:739–47.

Guha S.K. and Chattopadhyay A.K., 2007. On the linear stability analysis of finite hydrodynamic porous journal bearing under coupled stress lubrication. J Eng Tribol IMECHE, **221**:831–840.

Guha S.K., 2010. Linear stability performance analysis of finite hydrostatic porous journal bearings under the coupled stress lubrication with the additives effects into pores. Tribology International, **43**:1294–1306.

Beavers G.S. and Joseph D.D., 1967. Boundary conditions of a naturally permeable wall. J Fluid Mech., **30**:197– 207.

Darcy H., 1856. Les Fontaines Publiques de la Ville de Dijon, Dalmont, Paris.